The Dispersion of Discrete Particles in a Turbulent Fluid Field

RICHARD V. CALABRESE
and
STANLEY MIDDLEMAN
Department of Chemical Engineering
University of Massachusetts
Amherst, MA 01003

The degree of radial dispersion of medium size particles ($\eta_K < d_p < l_f$) emanating from a point source, is measured photographically in the turbulent core of a fully developed vertical pipe flow of water. From the classical theoretical results of G. Taylor, it was then possible to calculate statistical parameters which characterize the turbulent particle motion. A comparison is made between a tracer and neutrally dense, buoyant and heavy particles. Results indicate that the effect of particle inertia is negligible, and that the crossing trajectories effect dominates the dispersion process. A "wake effect" causes a buoyant particle to disperse to a greater degree than an equivalent heavy particle. An exponential-cosine form of the Lagrangian autocorrelation coefficient provides a best fit for the dispersion data, although a purely exponential form is equally adequate for practical calculations.

SCOPE

The degree of dispersion of discrete particles in a turbulent fluid field is affected by particle size, inertia, free fall velocity, and relative density, as well as by the underlying fluid turbulence. Very little data exist which report the relative contributions of these parameters to the dispersion process and the statistical parameters which describe the particle motion. Previous experimental studies have been limited to very small particles (Snyder and Lumley 1971) and to very large particles (Howard et al. 1973). Here, we experimentally examine the degree of radial dispersion of a dilute suspension of neutrally dense, buoyant and heavy, medium size particles in the turbulent core of a fully developed vertical pipe flow of water, using a photographic technique. A medium size particle is one whose diameter is larger than the Kolmogorov fluid microscale, but smaller than the integral scale.

Turbulence parameters were estimated from the radial dispersion data, using dispersion models developed from the classical theory of G. Taylor (1921), by assuming several functional forms of the Lagrangian autocorrelation, and by employing a nonlinear least squares regression technique. The resulting turbulence parameters are used to calculate Lagrangian energy spectra for the various particles. Tracer dispersion data and estimated fluid turbulence parameters, obtained in the same experimental facility by A. Taylor and Middleman (1974), provide a basis for comparison. The approximate range of variables studied is $0.25 < d_p/l_f < 0.50$; $0.25 < \tau_p/T_{L_f} < 0.50$; and $0 \leq |f|/u'_f < 3.3$. The particle relaxation time, τ_p, is a measure of particle inertia. The magnitude of the free fall velocity, f, is a measure of the crossing trajectories effect. A "wake effect" which causes a buoyant particle to be convected upwards into its own wake in a downward directed mean flow, is also considered. Resulting particle turbulence parameters are compared with the small particle data of Snyder and Lumley (1971).

CONCLUSIONS AND SIGNIFICANCE

Through the experiments described, it was possible to obtain reliable measurements of particle turbulence parameters. Results indicate the following conclusions can be drawn for the range of variables studied:

1. The degree of radial dispersion of a neutrally dense medium size particle ($\eta_K < d_p < l_f$) does not differ appreciably from that of a tracer.
2. Neither particle size nor inertia contribute significantly to the degree of radial dispersion of a medium size particle.
3. The effect of crossing trajectories is to decrease the degree of radial dispersion of a medium size particle, relative to that of a tracer.
4. The "wake effect" causes a buoyant particle of medium size to have a larger degree of dispersion than an equivalent heavy particle, in a downward directed mean flow.
5. As the effect of crossing trajectories increases, the Lagrangian integral time and length scales, and the eddy diffusivity of a medium size particle, decreases.
6. As the effect of crossing trajectories increases, there is a reduction in turbulent energy at lower frequencies. The range of energy containing frequencies is displaced towards the higher end of the energy spectrum.
7. An exponential-cosine, $m = 1$ form of the Lagrangian autocorrelation coefficient best describes the decay of the particle radial turbulent velocity field, although for practical applications an exponential form is equally adequate.
8. The calculated medium size particle turbulence parameters of this study compare favorably with the directly measured small particle data of Snyder and Lumley (1971).

Direct correspondence to R. V. Calabrese, Pickard, Lowe, and Garrick, Inc., Suite 612, 1200 Eighteenth Street, N.W., Washington, DC 20036. Stanley Middleman is presently at Department AMES, B-010, University of California, San Diego, La Jolla, California 92093.

0065-8812-79-3092-1025-$01.10. © The American Institute of Chemical Engineers, 1979.

If one is interested in predicting the spread of soot from an industrial source into the atmosphere, the dispersion of silt and solid contaminants in rivers, or the deposition of particles from a moving stream onto horizontal or vertical surfaces, one must have a knowledge of the motion of these particles relative to the turbulent carrier fluid. An understanding of the forces affecting particle dispersion and deposition is also important in bounded flows. Examples are the transport of suspended solids through pipes, the motion of catalyst pellets in fluidized and moving bed reactors, and the movement of solid wastes in a fluidized bed incinerator.

The aforementioned turbulent flows are inhomogeneous and anisotropic, and considering particle dispersion in these complex flow fields would not yield fundamental information about fluid-particle interactions. A more realistic approach is to look at the motion of a very dilute suspension of spherical particles in a simple flow, in which the characteristics of the turbulent fluid field are well understood. This information can then be applied to the complex real situations. Such a flow field is the core region of a fully developed pipe flow of water.

PHYSICAL BACKGROUND

Consider the motion of a single spherical particle in a homogeneous and isotropic turbulent field. The path traveled by the particle will differ from that of a fluid point due to the characteristic properties of both the particle and the turbulent fluid field. If the particle is small compared to the smallest scale of turbulent motion (Kolmogorov or microscale), particle dispersion will be influenced by the entire spectrum of eddy sizes and the particle will see a uniform velocity field during its residence time within an eddy. The inertia of the particle, characterized by a particle relaxation time, will cause its root mean square (rms) fluctuating velocity to be less than that of a fluid point, due to drag at the fluid-particle interface. The extent to which the rms particle velocity will differ from that of the fluid depends on the relative magnitudes of the particle relaxation time and some characteristic time scale of the turbulence.

It is not clear whether the fluid time microscale or Lagrangian integral scale is the proper scaling parameter for particle inertia. Snyder and Lumley (1971) argue for the former, while Meek and Jones (1973) say it should be the latter. However, as the particle inertia increases, it will respond more slowly to the fluctuating fluid motions. If the particle relaxation time is small compared to all fluid time scales, the particle will be able to respond to the entire fluid frequency spectrum. The drag at the fluid-particle interface increases the time during which the particle velocity will be correlated with its previous motion. Therefore, for particles whose size and relaxation time are small compared to the respective turbulence microscales, the effect of increasing inertia is to increase the particle integral time scale and decrease its rms fluctuating velocity. This sort of physical reasoning has been confirmed theoretically by many authors (Soo 1956, Chao 1964, Meek and Jones 1973, among others). The effect on particle dispersion is not obvious since, according to the statistical theory of turbulent dispersion, the degree of dispersion is determined from the product of the mean square fluctuating velocity and the integral time scale. The reader is referred to the recent work of Reeks (1977) and Pismen and Nir (1978).

If a particle has appreciable free-fall velocity, it will not remain within an eddy, but will migrate from one to another. It is possible to define a free-fall time scale which characterizes the rate at which the particle migrates through the turbulent field. If this time is larger than the time microscale, the particle will not have sufficient time to respond to the higher frequency components of the turbulent fluid field. Note that the characteristic free-fall time is related to the particle inertial relaxation time and in some cases is the same. This will be discussed later.

For now, let us confine our discussion to particles whose free-fall response time is small, compared to the Kolmogorov scale. Since the turbulent field is homogeneous, the particle will experience the same distribution of turbulence states during its migration as it would if confined within one eddy. In the one case, the particle experiences the distribution of turbulence states by remaining within an eddy which undergoes the distribution during its lifetime. In the other case, the particle experiences the turbulence by moving from one region of correlated fluid to another. The time scales of correlation are different, due to differing convection velocities. The resulting loss of correlation (decrease in the particle integral time scale) depends on the relative magnitudes of the free-fall velocity and a characteristic rms fluctuating velocity for the system.

It is not clear whether this velocity should be that of the particle or the fluid. The work of Meek and Jones (1973) and Reeks (1978) seems to point to the former. Their analyses, however, show that the rms particle velocity can be calculated from the particle free-fall velocity and fluid scales. The effect of particle free fall was first considered by Yudine (1959) and is known as the "crossing trajectories" effect. Its influence is opposite to that of inertia on the particle integral time scale.

Very little information exists concerning the relative contributions of inertia and crossing trajectories to the motion of small particles. Experimental data are particularly lacking. The reader is referred to the theoretical work of Csanady (1963), Meek and Jones (1973) and Reeks (1978).

Before going further, let us define a small particle as one whose diameter is less than the fluid microscale, a large particle as one whose diameter is larger than the fluid integral scale, and a medium particle as one whose size lies between these two. These definitions are somewhat ambiguous, since it is possible to have a small particle whose inertial relaxation time is greater than the time microscale, etc. They will, however, suffice for the discussion that follows.

For a small particle, the effect of particle inertia and crossing trajectories is further complicated if the characteristic time for either or both of these phenomena is larger than the time microscale. Although the particle will not disturb the turbulent fluid field, it will not respond to the higher frequency components of the eddy spectrum. If the particle is sufficiently dense, it will behave like a projectile as it cuts through the turbulent field.

When the particle is larger than the smallest turbulence dimensions, the fluid-particle interactions are extremely complex. Very little information exists, and any proposed mechanism of fluid-particle interaction must be viewed with caution. Laboratory data are scarce and those which exist appear to be physically unappealing. The purpose of the following discussion is to explain rather than make definitive statements concerning the complex physical situation.

As particle size increases beyond the Kolmogorov scale, the small scale fluid structure becomes increasingly ineffective in influencing particle dispersion. Not only does the influence of the higher wave number components decrease, but the small scale structure may itself be altered

by the presence of the particle. If the particle is large, it can at most respond to the very slow large scale motion. Consider a particle of medium size. If it encounters an eddy considerably smaller than its diameter, it will probably dissipate or completely alter the structure of the eddy. If the particle encounters an eddy much larger than itself, it will see a uniform velocity field during its residence time within that eddy, and its response to that velocity field will be governed by its inertia.

A most complex situation exists when the particle encounters an eddy whose size does not differ appreciably from its own. In this case, the manner in which the fluid and particle interact will depend on the mode of encounter. For instance, if the eddy brushes against the particle, it may push it away, into another correlated region. The eddy structure may or may not be altered. If the eddy confronts the particle directly, it may be partially or totally dissipated, depending on the degree of contact. The fluid-particle interactions in this size range are not reproducible, and the process of particle-eddy encounter is not deterministic. We have a situation where the turbulent fluid field is homogeneous and statistically stationary, but a portion of the turbulent particle field is statistically nonstationary. Unfortunately the tools developed to date to extract fundamental information about turbulence are only strictly valid for a stationary field.

Our discussion ignores the contributions of particle inertia and free fall when the associated time scales for these phenomena are larger than the time microscale. The contributions of particle size, inertia, and crossing trajectories are interrelated and are too complex to expound upon clearly. These simultaneous effects probably broaden the range over which non-reproducible interactions can occur.

In addition to determining particle inertia and free fall velocity, the relative density between particle and fluid plays another important role in the dispersion of medium and large particles. If a particle is large enough to shed a wake whose dimensions are larger than the microscale, how this wake will affect the particle motion and alter the flow field in the vicinity of the particle depends on the relative density. For instance, if the mean fluid velocity is directed vertically downward, a dense particle ($\rho_p > \rho$) will tend to migrate ahead of the mean fluid motion, shedding its wake "behind" and away from itself. However a buoyant particle ($\rho > \rho_p$) will tend to migrate upward shedding its wake "in front" of itself. If the particle rising velocity is smaller than the mean fluid velocity, the particle may be convected into its own wake. Therefore, a heavy particle and a light particle of equal inertia and absolute value of free-fall velocity will not necessarily behave in a similar manner in the same fluid field. The heavy particle will appear to be sluggish, while the buoyant one will appear to be oversensitive. The opposite situation will occur if the mean flow is directed vertically upward. We will henceforth refer to this phenomenon as the "wake effect."

In summary, how a particle will respond in a turbulent field depends on its relative density, size, inertia, and free fall velocity, as well as the structure of the fluid field.

RELATED LITERATURE

A detailed presentation of previous work will not be attempted here. Only the more relevant studies will be mentioned. Calabrese (1975) presents an extensive review of previous work, in the dissertation from which this paper is extracted.

Via statistical theory, several authors have derived models which relate particle turbulence parameters to those of the fluid. Among them are works of Soo (1956), Liu (1956), Friedlander (1957), Tchen (1959), Csanady (1963), Chao (1964), Shirazi (1967), Meek and Jones (1973), Reeks (1977), and Pismen and Nir (1978). Their findings are consistent with the physical ideas put forth above. Some have shown that a particle can exhibit anisotropic behavior in an isotropic fluid field. However, all theoretical work to date has been limited to small particles which follow a linear (Stokes) drag law. In addition, it was necessary to assume a functional form for the fluid eddy spectrum.

Most of the experimental work to date has focused on the measurement of particle diffusivity only. Householder and Goldschmidt (1969) present a thorough review of previous tracer and particle experiments. In a more recent study, Sharp and O'Neil (1971) found that for large particles, particle diffusivities were much larger than that of the fluid. This is true for all large particle studies.

Kennedy (1965) measured the dispersion of medium size particles in the grid-generated turbulence of a vertical wind tunnel. Turbulent intensity and eddy diffusivity were calculated, respectively, from the initial and final slopes of the decay-corrected dispersion data, so accuracy is considered poor. Snyder and Lumley (1971) have severely criticized this work.

Jones (1966) and Shirazi (1967) studied the dispersion of large particles in water, in the core of a fully developed pipe flow, using an optical light sensing technique. Particle velocities could be inferred by measuring the instantaneous particle position. Their data show that a large dense particle can have a higher rms velocity than the fluid in which it is moving. Since their data are plagued by noise, they declined to explain this seemingly unappealing result. Howard et al. (1973) perfected the University of Illinois facility used by Jones and Shirazi, by improving the electronics and by radioactive tagging of the particles. According to Jones (1978), these data will be reported soon, and a large dense particle can, indeed, have a higher rms velocity than the fluid. It should be kept in mind that in most studies, the rms fluid velocity is measured in the absence of particles. We will consider this point later.

The most sophisticated experimental study reported to date is that of Snyder and Lumley (1971). Using a photographic technique, they obtained direct measurements of the particle autocorrelation function for small heavy particles in an experimental facility identical to that of Kennedy (1965). Details of the experimental technique, as well as a complete error analysis, are given by Snyder (1970). For the particles studied, inertia and crossing trajectories are inseparable. The particle intensity decreases as particle inertia and free-fall velocity increases, and in all cases is less than the measured Eulerian fluid intensity. The particle integral time scale, which is evaluated from the decay-corrected data, decreases as particle inertia and free-fall velocity increases, indicating the predominance of the crossing trajectories effect. The particle autocorrelations have the same functional form as the Eulerian spatial fluid autocorrelation and exhibit negative loops, as is expected for dispersion in a direction perpendicular to the mean fluid velocity field.

Meek and Jones (1973) reinterpreted Snyder and Lumley's data to show that they are consistent with their theory and that both particle inertia and crossing trajectories are important in determining the particle turbulence parameters.

THEORY

The statistical description of tracer dispersion from a point source in a homogeneous turbulent flow was first given by G. Taylor (1921). The fundamental result relates the mean square displacement $\overline{X^2}$ to the mean square fluctuating velocity $\overline{u^2}$ in the direction transverse to the mean flow, and to the Lagrangian velocity correlation coefficient $R_L(\tau)$

$$\overline{X^2} = 2\overline{u^2} \int_0^t \int_0^{t'} R_L(\tau)\, d\tau\, dt' \tag{1}$$

The correlation coefficient is defined by

$$R_L(\tau) = \frac{\overline{u(t)\, u(t-\tau)}}{\overline{u^2(t)}} \tag{2}$$

Although Taylor applied his theory to the dispersion of fluid points, Snyder and Lumley (1971) show that it can be applied to particle dispersion, provided that all quantities are interpreted as belonging to the particle.

For small time, it can be seen that $R(\tau)$ approaches unity, from which it follows that

$$\lim_{t \to 0} \overline{X^2} = \overline{u^2}\, t^2 \tag{3}$$

For long times, the velocity fluctuations become uncorrelated, and it is possible to define a Lagrangian integral time scale T_L as

$$T_L = \int_0^\infty R_L(\tau)\, d\tau \tag{4}$$

Using Equation (4) with Equation (1), it is possible to show that

$$\lim_{t \to \infty} \overline{X^2} = 2\overline{u^2}\, T_L\, t \tag{5}$$

By analogy to Einstein's (1905) formulation of diffusion by Brownian motion, Taylor defined a turbulent diffusivity by

$$E_D = \frac{1}{2} \frac{d\overline{X^2}}{dt} \bigg|_{t \to \infty} = \overline{u^2}\, T_L \tag{6}$$

From Equations (3) and (6), and upon examining mean square displacement data for a tracer or particle at very short times and very long times, it is possible to determine both $\overline{u^2}$ and T_L. $R_L(\tau)$ can be determined by double differentiation of the dispersion data for all times, as indicated by Equation (1).

Because short-time point source dispersion data are usually inaccurate and differentiation of data leads to inaccuracies, estimates of $\overline{u^2}$, T_L, and $R_L(\tau)$, obtained as indicated above, are usually poor. One means of circumventing such a problem is to assume several functional forms for the correlation coefficient. Equation (1) can then be integrated analytically, and estimates of $\overline{u^2}$ and T_L can be obtained from the resulting models, using a suitable nonlinear regression technique. Parameter estimates from the resulting models can be compared via some best fit criteria to determine which functional form for $R_L(\tau)$ best describes the dispersion process.

A class of semi-empirical expressions for $R_L(\tau)$ was proposed by Frenkiel (1953) to describe the motion of fluid points

$$R_L(\tau) = \exp\left[\frac{-\tau}{(m^2+1)T_L}\right] \cos\left[\frac{m\tau}{(m^2+1)T_L}\right] \tag{7}$$

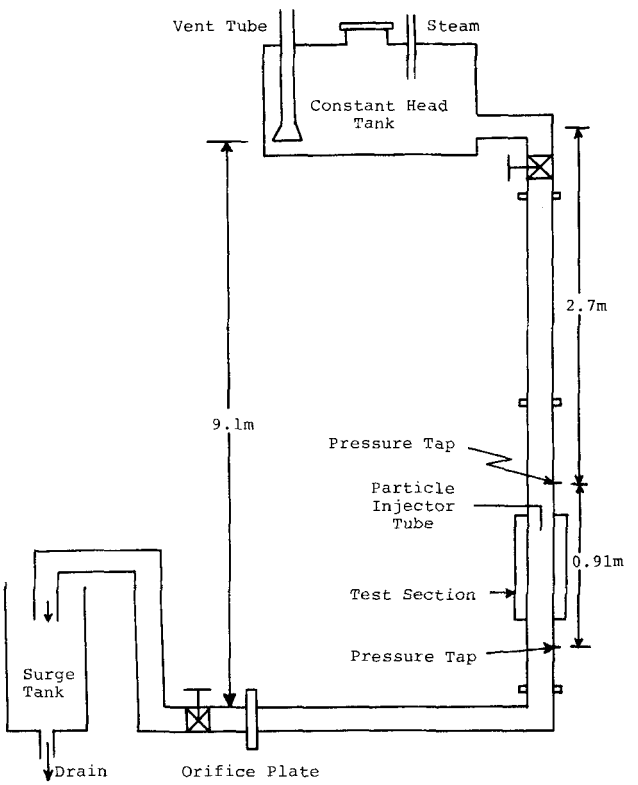

Figure 1. Schematic of apparatus.

where m can be zero or a positive integer. For $m \geq 1$, Equation (7) satisfies the theoretical criteria set forth by Hinze (1959), and the physical restriction set forth by Tennekes and Lumley (1972) (that the correlation coefficient in the direction transverse to the flow must exhibit negative loops). When $m = 0$, Equation (7) predicts simple exponential decay, a physically and theoretically invalid process. Nevertheless, Equation (7) with $m = 0$ has been used successfully by several authors. Kennedy (1965) and Snyder and Lumley (1971) show that the form of the non-dimensional particle correlation is the same as that for fluid points. Therefore Equation (7) can be applied to particle dispersion data, and substituted into Equation (1) to obtain a set of models for both particle and tracer dispersion. Discrimination among the different models ($m = 0, 1, 2, 3$, etc.) is made by comparing the error variance σ^2 for each model

$$\sigma^2 = \sum_i^n [\overline{X^2}_{\text{exp}} - \overline{X^2}_{\text{model}}]_i^2 / (N - P) \tag{8}$$

where N is the number of data points and P is the number of estimated parameters. Here $P = 2$, the parameters being $\overline{u^2}$ and T_L. A. Taylor and Middleman (1974) successfully applied this approach (with $m = 0, 1$) to tracer dispersion data.

Once the Lagrangian turbulence parameters are known, the microscales can be calculated from an estimate of the dissipation rate. For isotropic turbulence in a Newtonian fluid, G. Taylor (1935) found the rate of viscous dissipation to be

$$\epsilon = 15\, \nu\, \overline{u^2}/\lambda^2 \tag{9}$$

According to A. Taylor and Middleman (1974)

$$\lambda^2 = 24\, \nu\, T_L \tag{10}$$

Equations (9) and (10) can be combined to yield

$$\epsilon = \frac{5}{8}\frac{\overline{u^2}}{T_L} \qquad (11)$$

Equation (11) applies strictly to a fluid, but can also be applied to a particle for qualitative comparisons. The Kolmogorov length η_K and time t_K microscales are estimated from

$$\eta_K = (\nu^3/\epsilon)^{1/4}; \quad t_K = (\nu/\epsilon)^{1/2} \qquad (12)$$

Another means of comparing the motion of particles or fluid points is in terms of the Lagrangian energy spectrum function $E_L(\omega)$, defined as the Fourier transform of $R_L(\tau)$

$$E_L(\omega) = 4\overline{u^2}\int_0^\infty R_L(\tau)\cos(2\pi\omega\tau)\,d\tau \qquad (13)$$

Equation (7) can be substituted into Equation (13) to yield a model for calculating $E_L(\omega)$, using the best estimates of $\overline{u^2}$ and T_L.

Equations (1) through (13) afford a method by which tracer and particle dispersion data can be analyzed and compared, and estimates of turbulence parameters obtained.

EXPERIMENTS

A schematic drawing of the experimental system is shown in Figure 1. A large constant head reservoir feeds water to a 5.28 cm I.D. transparent acrylic pipe, which descends vertically to the floor below. The system was designed and constructed for the dye tracer experiments of A. Taylor and Middleman (1974). Some modifications were necessary for the present study. The details of the design are given by A. Taylor (1974) and the modifications by Calabrese (1975). Taylor's friction factor data show that fully developed flow conditions exist at distances greater than 50 pipe diameters from the constant head tank. Use of this system allows comparison of the results of this study with the tracer data of Taylor and Middleman (1974).

Following the work of Grant and Middleman (1966), Scheele and Meister (1968), and Fenn and Middleman (1969), we introduced a dilute point source of particles of fairly uniform size, by breaking up a laminar jet of an immiscible liquid of the desired density. The particle fluid is passed from a dispensing vessel, through a micrometering valve, to the 0.159 cm stainless steel particle injector tube. Since we had to introduce the particles isokinetically, drop size was controlled by cementing smaller stainless steel capillary tubes into the tip of the injector tube. For some of the experiments, deviations from isokinetic entry was necessary to maintain a uniform, continuous particle source.

A mathematical model developed from the equation of motion for a particle (Soo 1967), reveals that no appreciable error was introduced. Photographic observations show that the particles always remained spherical. Comparing these with the data of Middleman (1974) reveals that none of the particles break up in the flow field and that internal circulations do not exist. An analysis of the resulting data reveals that the injector tube did not disturb the flow field and that the method of particle generation and injection produced a point source of particles, 5 to 10 diameters apart, from which accurate mean squared displacement data can be obtained. The details are given by Calabrese (1975).

Data were recorded photographically. We used a 35 mm Nikon F2 camera, equipped with a 55 mm Micronikor lens, and an Angus Model 1272 automatic thyristor circuit flash. The flash duration was approximately 3×10^{-5} sec, sufficiently fast to freeze the particle motion. To insure maximum contrast, we dyed the particle fluids with Sudan blue (an organic dye insoluble in water, manufactured by GAF) and equipped the camera with an orange filter. The film was Kodak TRI-X. For determining particle size and distribution, the camera had an extension tube for high magnification. The magnification

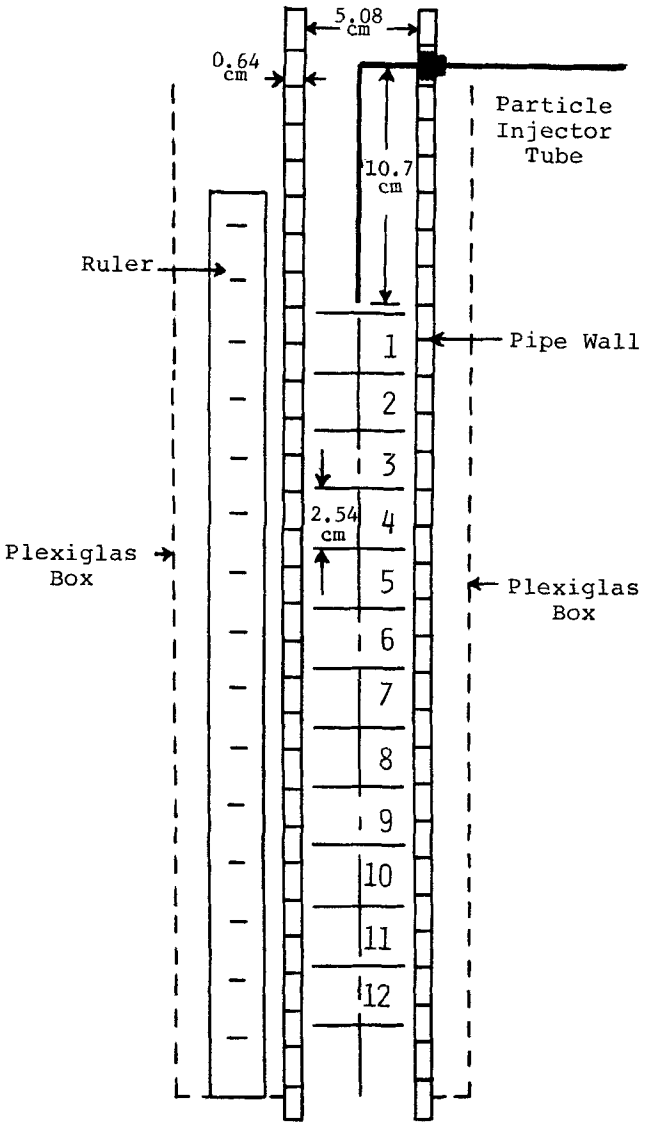

Figure 2. Test section.

factor was determined by simultaneously photographing the particles and the injector tube.

A schematic diagram of the test section, located 51 to 60 pipe diameters downstream of the constant head tank valve, is shown in Figure 2. It is divided into 12 sections, each 2.54 cm long, and surrounded by a plexiglas box, containing a ruler. The box was filled with water to eliminate distortions in the photographs due to pipe curvature. The ruler showed the degree of magnification. Two sets of photographs were taken, one covering stations 1 to 6 and the other, stations 7 to 12. A preliminary experiment was conducted with a mirror replacing the ruler. With proper alignment of the mirror, particle mean square displacement is perpendicular planes could be determined simultaneously. Within the limits of statistical error, the particle dispersion was axisymmetric.

Particle size and radial mean squared displacement were determined from at least 300 counts by projection of the negatives onto a screen. Displacement data were measured from the photographs for stations 1, 2, 3, 4, 6, 8, 10, and 12. Stations 5, 7, 9, and 11 were not analyzed due to the cumbersome nature of the data reduction technique. These stations were eliminated, since according to G. Taylor's (1921) theory, mean square displacement increases linearly at larger dispersion times. Following the work of Snyder and Lumley (1971), the parallax error and all other errors associated with data acquisition and measurement were considered and found to be small, compared to the standard error associated with predicting mean square displacement from a sample of finite

Table 1. Particle Parameters for Experimental Runs

Run No.	Particle fluid	Mean particle diameter, microns	Percent standard deviation	Inertial relaxation time, in sec	Free-fall velocity, cm/s
1	BB	862	12.1	.0615	<0.10
2	BB	584	15.1	.0283	<0.10
3	BB	842	12.0	.0588	<0.10
4	BB	945	11.3	.0739	<0.10
5	CCl_4	529	11.2	.0324	4.01
6	CCl_4	608	11.1	.0427	4.72
7	CCl_4	706	9.3	.0551	4.97
8	CCl_4	946	10.2	.0990	6.82
9	Hep	642	15.1	.0270	−3.25
10	Hep	809	13.7	.0428	−4.15

size (to be discussed later). Again the reader is referred to Calabrese (1975) for details of the above discussion.

METHOD OF DATA ANALYSIS

The radial mean square displacement about the pipe centerline was calculated from the particle position data at each station analyzed according to

$$\overline{X^2} = \sum_{i=1}^{n} X_i^2/n \qquad (14)$$

This is just the second moment of the displacement distribution. The standard error associated with predicting $\overline{X^2}$ from a finite sample is

$$E_{STD} = \left[\frac{\sum_{i=1}^{n} X_i^4/n - \left(\sum_{i=1}^{n} X_i^2/n \right)^2}{n-1} \right]^{1/2} \qquad (15)$$

Confidence intervals are estimated from

$$\overline{X^2} = \overline{X^2} \pm t_{n,(1-\alpha)100}\, E_{STD} \qquad (16)$$

where $t_{n,(1-\alpha)100}$ is the student's t value for a sample of size n at $(1-\alpha)100\%$ confidence. The first (mean displacement), third (related to the skewness) and fourth (related to the kurtosis) moments of the distribution were also calculated. These moments, which provide a check on the symmetry of the distribution, revealed that particle dispersion was symmetric about the pipe centerline and that the particle displacement distribution is approximately Gaussian. For the sake of brevity, these moments will not be given here, but can be found in Calabrese (1975).

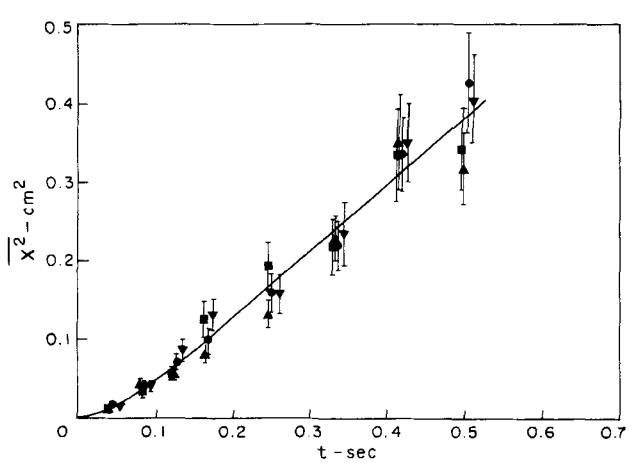

Figure 3. Comparison of degree of dispersion of neutral density (BB) particles; error bars indicate 95% confidence intervals; best fit curve derived from exponential-cosine, $m = 1$ model; ● $d_p = 584$ μm; ▽ $d_p = 842$ μm; ▲ $d_p = 862$ μm; ■ $d_p = 945$ μm.

Since the dispersion process has been confined to the core region of the flow field, the mean axial particle velocity is given by $\overline{U}_p = \overline{U}_0 + f$. If the turbulent velocities and the free-fall velocity are small compared to $\overline{U}_0$ (as is the case here), the dispersion time is given by $t = Z/\overline{U}_p$, where Z is the axial distance from the point source to the middle of the station of interest.

An expression for the particle inertial relaxation time, τ_p, can be obtained by non-dimensionalization of the dynamic equation describing the mean motion of a particle in a turbulent field. According to Lumley (1957)

$$\tau_p = (1 + 2\rho_p/\rho)\, d_p^2/36\nu \qquad (17)$$

A derivation of Equation (17) is also given by Calabrese (1975). It should be noted that "inertia" in this context involves more than a density difference between the particle and the surrounding fluid. Inertia exists because of the finite size of the particle, even when $\rho_p = \rho$.

The particle free-fall velocity can be calculated using the method of Heywood (1962). It is therefore possible to obtain quantitative measures of particle inertia, from Equation (17), and the effect of crossing trajectories, from f.

RESULTS

Ten experiments with particles of different density and mean diameter were performed at 21°C and a pipe Reynolds number of 24,500. A. Taylor and Middleman (1974) obtained tracer dispersion data in water at these conditions (in this experimental facility) and these data are used in this study. The particle fluids used are butyl benzoate (BB, $\rho = 1.000$ gm/cm^3), carbon tetrachloride (CCl_4, $\rho = 1.595$ gm/cm^3) and n-heptane (Hep, $\rho = 0.695$ gm/cm^3). BB is neutrally dense, CCl_4 is heavy, and Hep is buoyant with respect to water. Particle parameters for the experimental runs are summarized in Table 1. The particles are seen to have a narrow size distribution, as evidenced by small values of the percent standard deviation from the mean particle size. The neutrally dense BB particles have a small free-fall velocity, due to the slight difference between their density and that of water.

DISPERSION

The dispersion data are fit to dispersion models, as previously discussed, by substitution of Equation (7) into Equation (1) and subsequent use of the resulting equation with the Gaushaus (1966) non-linear least squares parameter estimation technique. The data for the four neutral density particle runs are presented in Figure 3. The error bars represent the 95% confidence intervals for the prediction of $\overline{X^2}$ from a finite sample. Within the limits of statistical error, the dispersion data for the four particle sizes are indistinguishable. This is also true at the 80% confidence level. The curve of Figure 3 represents the best fit line through all of the data based on the exponential-cosine, $m = 1$ model for $R_L(\tau)$ [Equation (7) with $m = 1$]. The best fit curves for the individual particles are not given, since they overlap and provide no additional information. Since neutrally dense particles do not exhibit a crossing trajectories effect, we conclude that the effect of inertia is negligible for the particle size range studied.

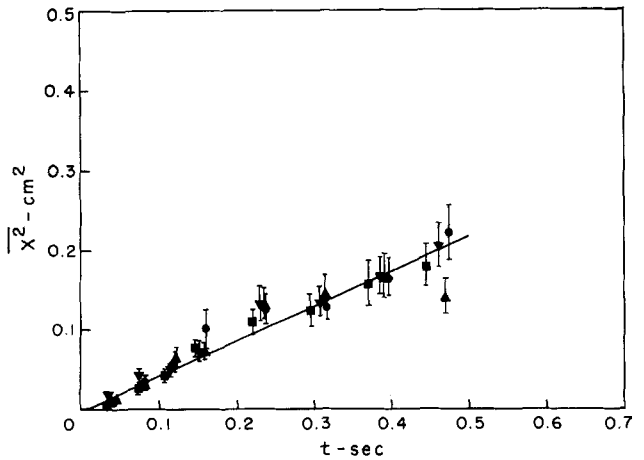

Figure 4. Comparison of degree of dispersion of heavy (CCl_4) particles; error bars indicate 95% confidence intervals; best fit curve derived from exponential-cosine, $m = 1$ model; ● $d_p = 529$ μm; ▲ $d_p = 608$ μm; ▽ $d_p = 706$ μm; ■ $d_p = 946$ μm.

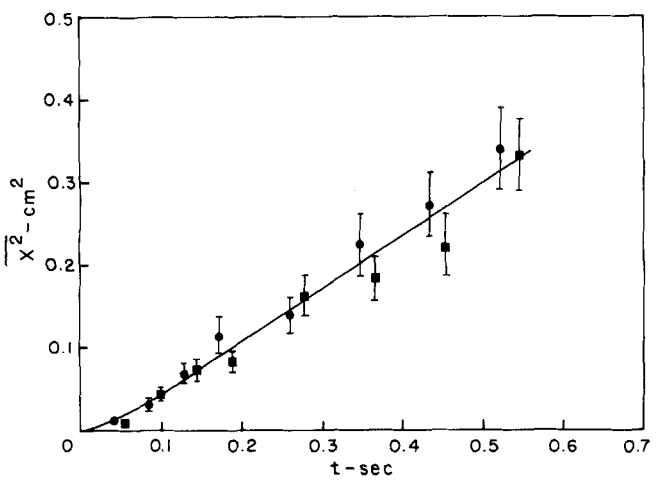

Figure 5. Comparison of degree of dispersion of buoyant (Hep) particles; error bars indicate 95% confidence intervals; best fit curve derived from exponential-cosine, $m = 1$ model; ● $d_p = 642$ μm; ■ $d_p = 809$ μm.

TABLE 2. ERROR VARIANCE* FOR BEST FIT OF MODELS

Model	Tracer	BB	CCl_4	Hep	Average
Exponential ($m = 0$)	2.80	5.48	3.28	4.09	3.91
Exponential-Cosine, $m = 1$	2.05	5.81	3.12	4.34	3.83
Exponential-Cosine, $m = 2$	1.48	6.33	1.89	6.38	4.02
Exponential-Cosine, $m = 3$	1.26	6.61	2.52	7.28	4.42
Exponential-Cosine, $m = 4$	1.17	6.78	3.40	7.75	4.78

* Values are $\sigma^2 \times 10^4$ cm^4.

Figures 4 and 5 show the dispersion data for the four heavy particle runs and the two buoyant particle runs, respectively. Again, within the limits of statistical error, it is not possible to distinguish among the four heavy particle runs and between the two buoyant particle runs. This is again true at 80% confidence, and the best fit lines are for all runs based on the exponential-cosine, $m = 1$ model. Comparing Figures 3, 4, and 5 reveals that the data for the different relative density groups are distinct. This is shown in Figure 6, where the best fit lines for the composite data (all runs) for each density group are compared with that obtained for the tracer by A. Taylor and Middleman (1974). For the particle size range studied, relative density governs the dispersion process. Also, the degree of dispersion of the tracer is a little larger than that of the neutrally dense particle, possibly due to a slight crossing trajectories effect.

The error variance for each of the five different dispersion models [Equation (7) with $m = 0, 1, 2, 3, 4$] is presented in Table 2. This supposed criterion for model discrimination does not distinguish among the models for the correlation coefficient. This is seen in Figure 7, which gives the best fit lines for all five models for the composite neutral density particle data. The dashed vertical line represents the longest time for which dispersion measurements were made. Longer time dispersion data are needed to use the σ^2 criterion for model discrimination.

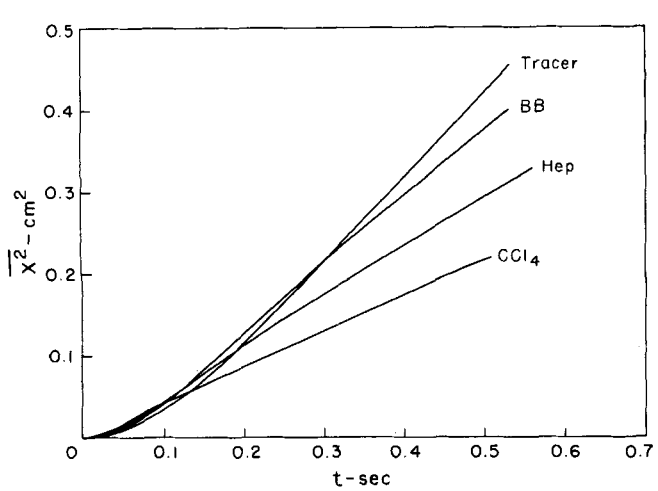

Figure 6. Comparison of degree of dispersion based on best fit curves—composite results; best fit curves derived from exponential-cosine, $m = 1$ model.

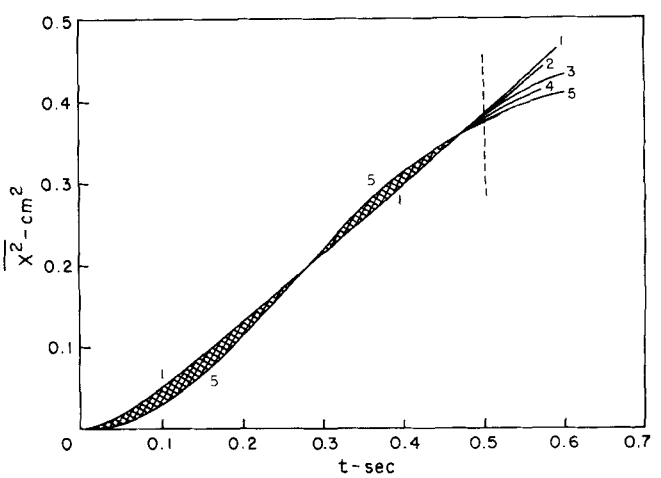

Figure 7. Comparison of dispersion models—composite neutral density (BB) particles; 1. Exponential ($m = 0$), 2. Exponential-cosine, $m = 1$, 3. Exponential-cosine, $m = 2$, 4. Exponential-cosine, $m = 3$, 5. Exponential-cosine, $m = 4$.

TABLE 3. DIMENSIONLESS DIFFUSIVITIES FOR TAYLOR'S TRACER DATA

Model	$a_D = E_D/D_p u_*$
Exponential	.0387
Exponential-Cosine, $m = 1$	.0310
Exponential-Cosine, $m = 2$	.0204
Exponential-Cosine, $m = 3$	.0144
Exponential-Cosine, $m = 4$	.0109

MODEL DISCRIMINATION

An alternate means for model discrimination will now be developed. A. Taylor and Middleman (1974) report tracer dispersion data in water at several Reynolds Numbers, in addition to $N_{Re} = 24{,}500$. These data can be fit to our models, and the turbulence parameters estimated, as discussed above. The predicted diffusivities can be combined with Taylor and Middleman's friction factor data, to predict dimensionless diffusivities defined by

$$a_D = E_D/D_p\, u_* \tag{18}$$

u_* is the friction velocity given by

$$u_* = \sqrt{F/2}\, \nu N_{Re}/D_p \tag{19}$$

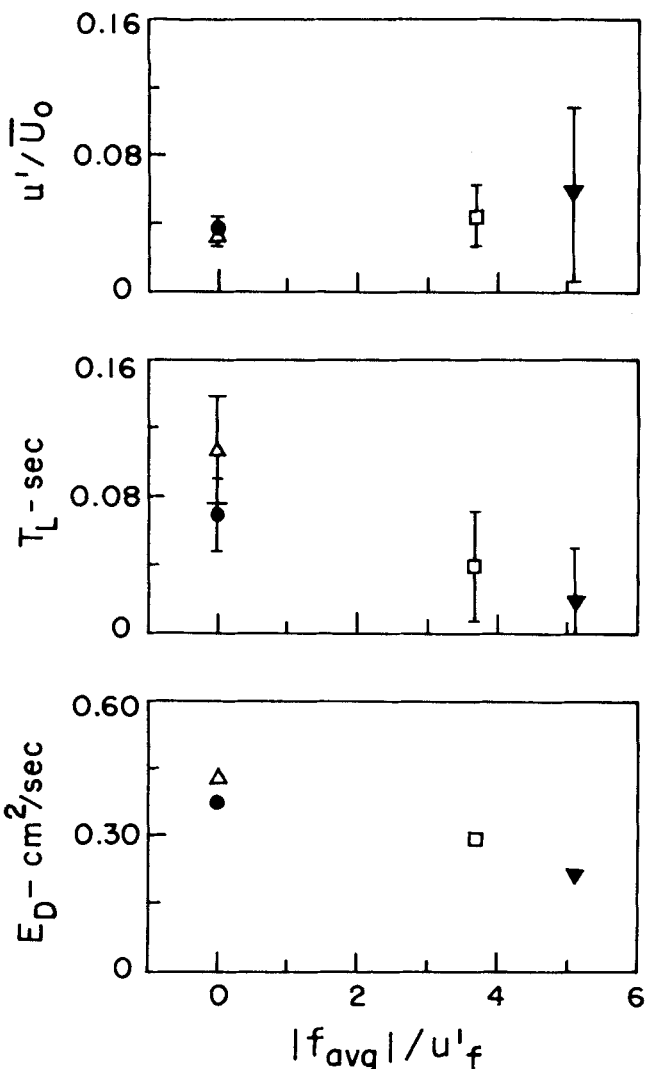

Figure 8. Composite turbulence parameters derived from exponential-cosine, $m = 1$ model; △ tracer; ● neutral density (BB); ▽ heavy (CCl_4); □ buoyant (Hep).

The average tracer diffusivities for all N_{Re} as predicted by our models are given in Table 3. It is well established (see Groenhof 1970; and Householder and Goldschmidt 1969) that the value of a_D for tracer dispersion in a pipe lies between 0.03 and 0.04. From Table 3, only the exponential model [Equation (7) with $m = 0$] and the exponential-cosine, $m = 1$ model give realistic estimates of a_D. Snyder and Lumley (1971) and Kennedy (1965) show that the form of $R_L(\tau)$ is the same for particle and tracer dispersion. Therefore we expect that only the $m = 0$ and $m = 1$ forms of Equation (7) will provide realistic estimates of the particle correlation coefficient. The exponential-cosine, $m = 1$ model satisfies all criteria for the form of $R_L(\tau)$. The exponential model is a theoretically and physically unrealistic model for transverse dispersion. As a result, the exponential-cosine, $m = 1$ model is favored, and will be considered the "best model" for subsequent analysis. Nevertheless, for practical calculations, the $m = 0$ and $m = 1$ forms of Equation (7) are equally acceptable.

TURBULENCE PARAMETERS

Since the degree of particle dispersion within a given relative density group is indistinguishable with respect to particle size, turbulence parameters are estimated for the tracer and the composite particle data for each density group. Turbulence parameters estimated from the exponential-cosine, $m = 1$ model are presented in Figure 8. Since the effect of inertia on particle dispersion is negligible for our data, the turbulence parameters are plotted against a measure of the crossing trajectories effect. This measure is taken as $|f_{avg}|/u'_f$. The magnitude of the average free-fall velocity for a given density group is $|f_{avg}|$. The turbulent intensity is $u' = \sqrt{u^2}$.

The magnitude of the crossing trajectories effect increases as both the particle size and relative density increase since both contribute to the free fall velocity. But the data show that the degree of dispersion is almost independent of particle size, and that small changes in free-fall velocity within a given relative density group are not important. Therefore the composite turbulence parameters should depend roughly on the relative density, or the average free-fall velocity for a given density group. The average free-fall velocity was chosen since it can be normalized with a characteristic rms velocity (see the discussion of the Physical Background section). The fluid

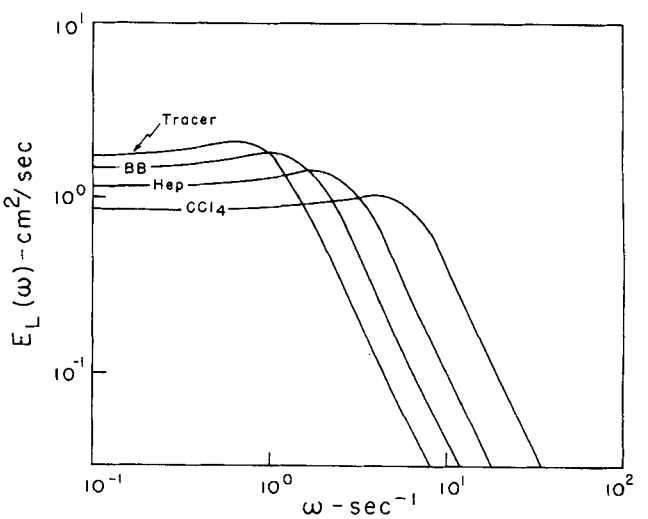

Figure 9. Composite energy spectra calculated from exponential-cosine, $m = 1$ model.

(tracer) intensity was chosen as the characteristic velocity, since the results show the particle intensities are unappealingly greater than the fluid intensity. We will discuss this point later. Figure 8 reveals that the particle integral time scale and diffusivity decrease, as the magnitude of the free-fall velocity increases. These results are consistent with the effect of crossing trajectories.

It is also of interest to examine the distribution of energy over frequency, as expressed by the energy spectrum function $E_L(\omega)$ given by Equations (13) and (7). The predicted energy spectrum functions with $m = 1$ in Equation (7) are given in Figure 9. As the effect of crossing trajectories increases, there is a reduction in turbulent energy at lower frequencies, and the range of energy containing frequencies is displaced farther towards the higher end of the spectrum.

DISCUSSION

For the range of experimental conditions studied, the inertial effect is negligible. The effect of crossing trajectories dominates the dispersion process and the exponential-cosine, $m = 1$ model best describes the decay of the velocity correlation. Fluid microscales based on this model are estimated from Equations (11) and (12). These are $\eta_K = 144$ microns and $t_K = 0.021$ sec. A rough estimate of the fluid Lagrangian integral length scale is given by $l_f = u'_f T_{Lf} = 2{,}180$ microns, where $T_{Lf} = 0.108$ sec. From Table 1, all particle sizes and response times τ_p lie between the fluid microscales and integral scales.

According to the data in that table, there is considerable overlap of the particle size distribution for the composite heavy and buoyant particle data of Figures 4 and 5, respectively. The neutral density particle data (Figure 3) reveal that the effect of particle size is negligible. Yet the dense and buoyant particles show distinct and different degrees of dispersion (Figure 6). This large difference cannot be attributed solely to the effect of crossing trajectories. The wake effect must be considered. Buoyant particles can be convected into their own wake by the mean fluid motion, causing them to appear "oversensitive," that is, their dispersion is enhanced by the particle-wake interaction. The turbulence parameters given in Figure 8 and the energy spectra of Figure 9 must be interpreted with this fact in mind.

The unappealing result that particle intensities are greater than that of the fluid has also been found by other investigators for large particles (Jones 1966, 1978, Shirazi 1977). But here and in other single particle or dilute suspension studies, the fluid intensity was measured in the absence of particles. Since medium and large particles can alter the fluid velocity field in their vicinity, the actual fluid intensity with particles present is not known. Consider a buoyant particle which exhibits a wake effect. Due to its rising velocity against the mean flow, it will tend to oscillate slightly in the flow field, imparting some of its momentum to, and accelerating, the fluid in its proximity. Therefore it is possible that the local fluid intensity is greater than that of the particle. One can imagine a large buoyant particle whose rising velocity is equal to the mean fluid velocity. In this case, the mean axial velocity of the particle will be zero, and the particle will oscillate vigorously in the pipe cross section.

A large heavy particle whose free-fall velocity is in the direction of the mean fluid velocity will have considerably more momentum than the surrounding fluid. As it cuts its way through the fluid field, it will not only alter its structure, but will impart some of its momentum to the fluid, causing it to accelerate locally. Again, the local fluid intensity is increased; and it is possible that the fluid intensity with the particle present is greater than the particle intensity and the fluid intensity in the absence of particles. In light of this discussion, the results of Figure 8 do not necessarily violate any physical principle. To fully resolve this conflict, it is necessary to simultaneously measure fluid and particle intensities. This

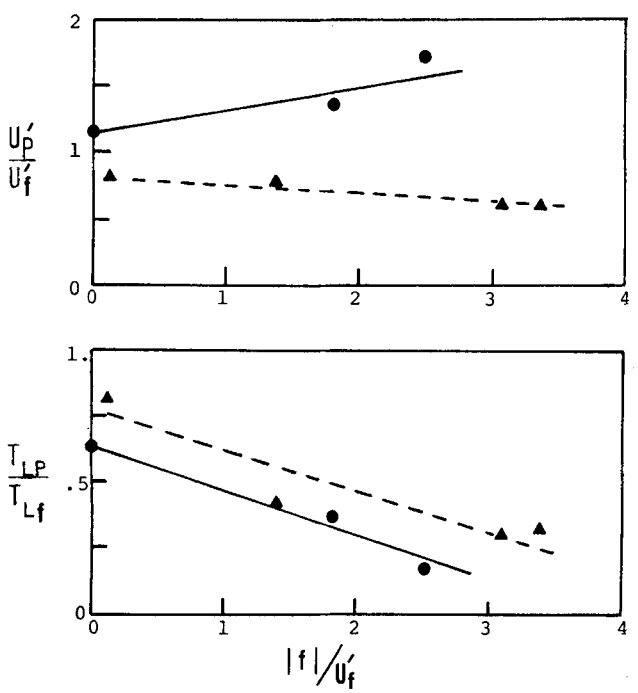

Figure 10. Comparison of results with data of Snyder and Lumley (1971); ● ——— present study; exponential-cosine, $m = 1$ model, ▲ - - - Snyder and Lumley (1971).

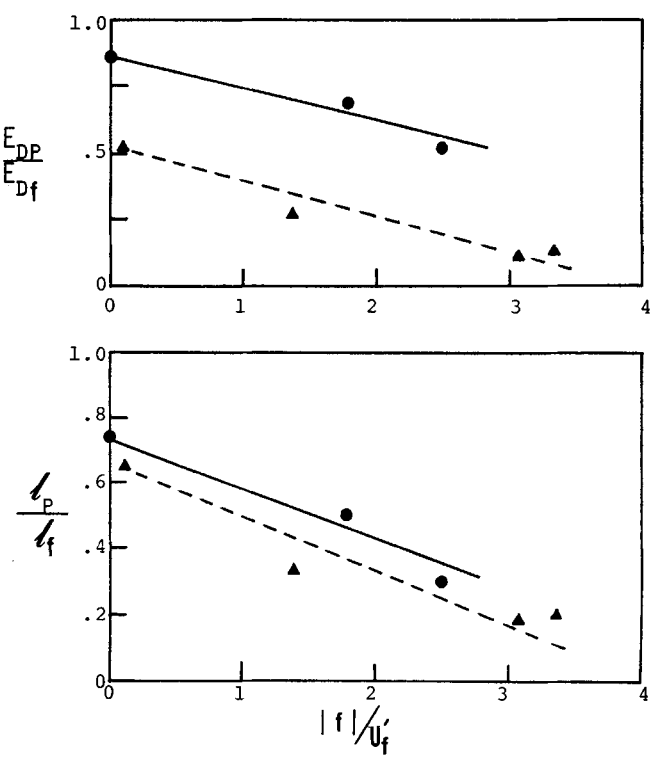

Figure 11. Comparison of results with data of Snyder and Lumley; ● ——— present study; exponential-cosine, $m = 1$ model, ▲ - - - Snyder and Lumley (1971).

has been done for dense suspensions of small particles by Soo, Ihrig, and El Kouh (1960).

An alternate interpretation of the data can be given in light of the fact that particle size alone does not influence the degree of dispersion. Consider a dilute suspension or cloud of particles of wide, but uniform, size distribution. A neutrally buoyant cloud will disperse to about the same degree as a tracer. A heavy cloud will exhibit less dispersion, and the degree of dispersion will decrease as the relative density between particle and fluid increases. This is due to crossing trajectories. A buoyant cloud of size distribution and relative density equal to that of the heavy cloud will disperse to a lesser degree than an equivalent neutrally dense cloud, but to a greater degree than the heavy cloud. This occurs because the effect of crossing trajectories is somewhat counteracted by the wake effect. For very large buoyant particles it is possible for the wake effect to completely dominate the dispersion process.

COMPARISON WITH DATA OF SNYDER AND LUMLEY (1971)

As previously mentioned, the most sophisticated experimental study to date is that of Snyder and Lumley (1971). They measured velocity autocorrelation functions and turbulence parameters for several small heavy particles, in the decay corrected turbulence of a vertical wind tunnel. Since these data represent the only unquestioned measurements of turbulence parameters in the literature, our results will be compared with their data, even though there is a difference in relative particle size.

Snyder and Lumley decay-corrected their results to values at $y/M = 73$, where y is the downstream distance from the turbulence producing grid and M is the grid mesh size. Therefore, the particle turbulence parameters for this distance will be used in the comparison. Fluid scales are needed to normalize the particle turbulence parameters. Snyder and Lumley measured the Eulerian fluid velocity field so the fluid intensity at $y/M = 73$ is available. The fluid integral time scale is obtained by extrapolating their particle integral scale data to zero inertia.

Since effects due to particle size and inertia are not important for the results of this study, the turbulence parameters are given as a function of f/u'_f. But the reader should keep in mind that the inertia effect *did* influence the results of Snyder and Lumley's study, although their results are crossing trajectories dominated. The comparison is made, using the turbulence parameters estimated from the exponential-cosine, $m = 1$ model, in Figures 10 and 11. The intensities show opposite trends, as expected, since the small particles of Snyder and Lumley's study should not influence the local fluid velocity field. The comparison between Lagrangian integral time scales is excellent, showing that the effect of crossing trajectories dominates particle motion in both studies. The integral time scales are less here than for Snyder and Lumley's experiments, since particle inertia, which tends to increase T_L, influenced their results. The eddy diffusivities for the two studies show the same trend, but the reduction in the degree of dispersion relative to a tracer is greater for the small heavy particles than for the medium size of this study. The comparison between integral length scales is again excellent. This is fortuitous since, although the turbulent intensities do not compare favorably, the products $u'T_L$ are in good agreement. The effect of crossing trajectories on particle integral scales and eddy diffusivity is similar for both small and medium size particles.

SUMMARY AND RECOMMENDATIONS

1. Nonlinear least squares regression analysis provides a convenient means to determine particle turbulence parameters from dispersion models, with relatively small amounts of dispersion data.
2. In general, an exponential-cosine, $m = 1$ form of the Lagrangian autocorrelation function best describes the decay of both the fluid and particle radial turbulent velocity fields. Still, the exponential form is equally acceptable for practical work. Turbulence parameters calculated from a dispersion model based on these forms of the autocorrelation are more realistic than those calculated from models based on exponential-cosine, $m > 1$ forms of the autocorrelation.
3. In the range of particle sizes studied, the degree of radial dispersion of a neutrally dense medium size particle does not differ significantly from that of a tracer.
4. Over the range of particle parameters studied, neither particle size nor inertia contribute significantly to the degree of radial dispersion of a particle.
5. The effect of crossing trajectories is to decrease the degree of radial dispersion of a medium size particle relative to that of a tracer.
6. The wake effect causes a buoyant particle of medium size to have a larger degree of dispersion than an equivalent heavy particle.
7. As the effect of crossing trajectories increases, the Lagrangian integral time and length scales, and the eddy diffusivity of a medium size particle decreases.
8. Calculated Lagrangian energy spectra for particles of medium size show that as the effect of crossing trajectories increases, there is a reduction in turbulent energy at lower frequencies, and the range of energy containing frequencies is displaced towards the higher end of the spectrum.
9. Data at longer dispersion times are needed in order to discriminate among models for the particle autocorrelation coefficient based on a best fit criterion, such as Equation (8).
10. Fluid and particle turbulence intensities should be measured simultaneously for dilute suspensions of medium and large particles, to establish the relationship between them.
11. Particle dispersion data at several pipe Reynolds numbers are needed over a wide range of particle parameters, to establish a correlation for practical engineering work.

NOTATION

a_D = dimensionless diffusivity
D_p = pipe diameter, cm
d_p = particle diameter, μm
$\overline{d_p}$ = mean particle diameter, μm
E_D = eddy diffusivity, cm^2/s
$E_L(\omega)$ = Lagrangian energy spectrum function, cm^2/s
E_{STD} = standard error, cm^2
F = friction factor
f = particle free-fall velocity, cm/s
f_{avg} = average free-fall velocity for a density group, cm/s
l = Lagrangian integral length scale, μm
m = constant in exponential-cosine analytical form of the Lagrangian autocorrelation coefficient defined by Equation (7)

N = number of observations of mean square displacement
N_{Re} = pipe Reynolds number
n = number of observations of particle diameter or particle displacement
P = number of parameters to be estimated by nonlinear regression
T_L = Lagrangian integral time scale, s
t = dispersion time, s
t_K = Kolmogorov time microscale, s
$\overline{U}_0$ = mean fluid centerline velocity in pipe, cm/s
$\overline{U}_p$ = mean particle velocity, cm/s
u = turbulent fluctuating velocity, cm/s
u' = turbulent intensity or rms velocity, cm/s
u_* = pipe friction velocity, cm/s
$\overline{u^2}$ = mean square turbulent velocity, cm^2/s^2
X = component of radial displacement in plane seen by the camera, cm
$\overline{X^2}$ = mean square displacement in plane seen by camera, cm^2

Greek Letters

ϵ = turbulent dissipation rate, cm^2/s^3
η_K = Kolmogorov length microscale, μm
λ = Taylor length microscale, μm
ρ = fluid density, gm/cm^3
ρ_p = particle density, gm/cm^3
σ^2 = error variance, cm^4
τ = time interval, s
τ_p = particle inertial relaxation time, s
ν = fluid kinematic viscosity, cm^2/s
ω = frequency, s^{-1}

Subscripts

f = fluid
p = particle

LITERATURE CITED

Calabrese, R. V., "The Dispersion of Discrete Particles in a Turbulent Fluid Field," Ph.D. thesis, University of Massachusetts, Amherst (1975).

Chao, B. T., "Turbulent Transport Behavior of Small Particles in Dilute Suspension," Ostereichisches Ingenieur-Archiv., Sonderabdruck aus Bd., XVIII, Heft 1 und 2, p. 7 (1964).

Csanady, G. T., "Turbulent Diffusion of Heavy Particles in the Atmosphere," *J. Atm. Sci.*, **20**, 201 (1963).

Einstein, A., *Investigations on the Theory of Brownian Movement*, Dover (1950).

Fenn, R. W., III, and S. Middleman. "Newtonian Jet Stability: The Role of Air Resistance," *AIChE J.*, **15**, 379 (1969).

Frenkiel, F. N., "Turbulent Diffusion from a Non-Punctual Source," in *Advances in Applied Mechanics*, Vol. 3, Academic Press, New York (1953).

Friedlander, S. K., "Behavior of Suspended Particles in a Turbulent Fluid," *AIChE J.*, **3**, 381 (1957).

Gaushaus, Nonlinear Least Squares, University of Wisconsin Computer Center, UWCC ID No. C0017-00/S0017-00 (1966).

Grant, R. P., and S. Middleman, "Newtonian Jet Stability," *AIChE J.*, **12**, 669 (1966).

Groenhof, H. C., "Eddy Diffusion in the Central Region of Turbulent Flows in Pipes and Between Parallel Plates," *Chem. Eng. Sci.*, **25**, 1005 (1970).

Heywood, H., "Uniform and Non-Uniform Motion of Particles in Fluids," Symposium on the Interaction Between Fluids and Particles, London, p. 1 (1962).

Hinze, J. O., *Turbulence*, McGraw-Hill, New York (1959).

Householder, M. K., and V. W. Goldschmidt, "Turbulent Diffusion and Schmidt Number of Particles," Proc. A.S.C.E., Eng. Mech. Div., EM **6**, 1345 (1969).

Howard, N. M., C. C. Meek, and B. G. Jones, "Experimental Measurements of Particle Dispersion in Turbulent Flow," Turbulence in Liquids, 3rd Symposium University of Missouri at Rolla (September, 1973).

Jones, B. G., "An Experimental Study of the Motion of Small Particles in a Turbulent Fluid Field Using Digital Techniques for Statistical Data Processing," Ph.D. dissertation, University of Illinois (1966).

Jones, B. G., personal communication (1978).

Kennedy, D. A., "Some Measurements of the Dispersion of Spheres in a Turbulent Flow," Ph.D. dissertation, The Johns Hopkins University (1965).

Liu, V. C., "Turbulent Dispersion of Dynamic Particles," *J. Meteorology*, **13**, 399 (1956).

Lumley, J. L., "Some Problems Connected with the Motion of Small Particles in Turbulent Fluid," Ph.D. dissertation, The Johns Hopkins University (1957).

Meek, C. C., and B. G. Jones, "Studies of the Behavior of Heavy Particles in a Turbulent Fluid Flow," *J. Atmos. Sci.*, **30**, 239 (1973).

Middleman, S., "Drop Size Distributions Produced by Turbulent Pipe Flow of Immiscible Fluids Through a Static Mixer," *Ind. Eng. Chem. Process Des. Dev.*, **13**, 78 (1974).

Pismen, L. M., and A. Nir, "On the Motion of Suspended Particles in Stationary Homogeneous Turbulence," *J. Fluid Mech.*, **84**, 193-206 (1978).

Reeks, M. W., "On the Dispersion of Small Particles Suspended in an Isotropic Turbulent Fluid," *J. Fluid Mech.*, **83**, 529-546 (1977).

Scheele, G. F., and B. J. Meister, "Drop Formation at Low Velocities in Liquid-Liquid Systems," *AIChE J.*, **14**, 9 (1968).

Sharp, B. B., and J. C. O'Neil, "Lateral Diffusion of Large Particles in Turbulent Pipe Flow," *J. Fluid Mech.*, **45**, 575 (1971).

Shirazi, M. A., "On the Motion of Small Particles in a Turbulent Fluid Field," Ph.D. dissertation, University of Illinois (1967).

Snyder, W. H., "Some Measurements of Particle Velocity Autocorrelation Functions in a Turbulent Flow," Ph.D. dissertation, Pennsylvania State University (1970).

Snyder, W. H., and J. L. Lumley, "Some Measurements of Particle Velocity Autocorrelation Functions in a Turbulent Flow," *J. Fluid Mech.*, **48**, 41 (1971).

Soo, S. L., "Statistical Properties of Momentum Transfer in Two-Phase Flow," *Chem. Eng. Sci.*, **5**, 57 (1956).

Soo, S. L., *Fluid Dynamics of Multiphase Systems*, Blaisdell Publ., Waltham, MA (1967).

Soo, S. L., H. K. Ihrig, Jr., and A. F. El Kouh, "Experimental Determination of Statistical Properties of Two-Phase Turbulent Motion," Trans. A.S.M.E., *J. Basic Eng.*, **82**, 609 (1960).

Taylor, A. R., "Turbulent Dispersion in Drag Reducing Fluids," Ph.D. dissertation, University of Massachusetts, Amherst (1974).

Taylor, A. R., and S. Middleman, "Turbulent Dispersion in Drag Reducing Fluids," *AIChE J.*, **20**, 454 (1974).

Taylor, G. I., "Diffusion by Continuous Movements," Proc. London Math. Soc., Ser. 2, **20**, 196 (1921).

Taylor, G. I., "Statistical Theory of Turbulence, Parts I-IV," Proc. Roy. Soc., **A151**, 421 (1935).

Tchen, C. M., "Diffusion of Particles in Turbulent Flow," in *Advances in Geophysics*, **6**, Academic Press, New York, p. 165 (1959).

Tennekes, H., and J. L. Lumley, *A First Course in Turbulence*, M.I.T. Press, Cambridge (1972).

Yudine, M. I., "Physical Considerations in Heavy Particle Diffusion," in *Advances in Geophysics*, **6**, Academic Press, New York, p. 185 (1959).

Manuscript received December 22, 1978; revision received June 22, and accepted July 6, 1979.